

Simulation of the Working Diameter in 3-Axis Ball-end Milling of Free Form Surface

Abdulwahab MGHHERONY*, Balázs MIKÓ

Abstract. Free-form surfaces are used in many aspects of the industry. When machining these surfaces using three-axis ball-end milling, the tool's working diameter continuously changes, due to the change in the surface geometry which affects the surface quality. This change in working diameter occurs from one point to another and continues along the surface even in the case of a constant tool path. Using a simultaneous five-axis milling machine can solve the problem, however, this solution comes at a high cost and complexity. This paper gives insight into the calculation of the effective diameter at each point of the milled surface and presents the effect of the different parameters by simulation. The simulation applies the geometric method, based on the coordinate transformation of the intersection curve. The presented simulation approach ensures optimization method for both the cutting process and the tool path. The ultimate goal is to reduce the cutting speed change considering the change of the current working diameter by controlling the spindle speed point to point, resulting in a more homogeneous surface.

Keywords: ball-end milling; effective diameter; free-form surface; surface roughness; three-axis milling

1 INTRODUCTION

Free-form surfaces are widely used in many aspects like aerospace, automobile, consumer products, and the die/mould industry [1]. A ball-end mill is mainly used in machining this kind of surfaces. The extended product life, high machining precision, low cost of the manufacturing process and its ability to feed axially make using this tool essential in industry [2-4].

When using the ball-end tool, the cut is not done by the whole diameter; what is called effective diameter takes place here. The reason for that is the changing of the radius from cutting edges to another with respect to the tool's rotation axis. The change of effect diameter causes a change in cutting parameter [5].

The effective diameter is related to the depth of cut (a_p), nominal diameter and the surface slop. It increases with the increasing depth of cut. When the depth of cut equals the tool's radius, the effective diameter will be equal to the nominal diameter. However, in some finishing operations, the depth of cut ranges between 0.1 - 0.3 mm, thus the effective diameter will be lower than the nominal diameter [5]. This problem can be solved using simultaneous five-axis milling; however, this technology's cost and complexity can be a problem.

Many researchers studied the machined surface and the significant factors that affect the quality of the surface [6]. Fan [7] examines the change of cutting speed when machining sculptured surfaces using 3-axis ball-end milling and found that the cutting speed has a significant effect on the quality of the surface and the tool life. De Souza et al. [8] study the impact of the working diameter on the cutting force, chip removal and surface roughness, and point out that the higher cutting speed decreases the surface roughness. Wojciechowski et al. [9] investigate the effect of tool inclination on the working diameter in the case of ball-end milling, and point out that with a large working diameter, the surface roughness is minor, and it decreases with the increase of the cutting. İzol et al. [10] study the importance of milling strategies and indicate that the applied strategies have a more significant effect than the width of cut on the surface roughness. Buj-Corral et al. [11] study the surface at different slopes and find that conventional milling can be recommended at a high depth

of cut and high speed. In ascendant trajectories, conventional milling is recommended to reduce the surface's roughness, whereas climb milling is preferred in descendant trajectories. Belguith et al. [12] investigate the effect of the tool bending on the cutting force magnitude in ball-end milling, and they indicate that while increasing, the tool bending the uncut thickness decreases due to the diminution of the equivalent radius. Huo et al. [13] present a new method to generate tool paths machining freeform surfaces using a three-axis CNC machine depending on a preferred feed direction field. Seikh et al. [14] study the synergistic effects of cutting parameters on surface roughness in ball-end milling of oxygen-free high conductivity (OFHC) copper, and they indicate that the axial and radial depth of cut has the most significant effect followed by the feed rate.

The above literature review shows that the optimization procedures for the ball-end milling process mainly focus on surface quality, tool life and tool path planning. Therefore, there is a need to emphasize the importance of cutting depth and surface geometry as these factors have a direct effect on the working diameter which in turn affects the cutting speed and as a result the surface quality.

In this paper, a geometric approach is presented to calculate the effective diameter when finishing the free surface using a ball end tool. The aim is to calculate the working diameter along the surface and to study the effect of surface inclination angles, axial and radial depth of cut and feed direction on the working diameter. For this purpose, a Matlab simulation was used to demonstrate the change in working diameter as a function of the above-mentioned factors.

2 EFFECTIVE DIAMETER

The nominal and the working, or effective diameter is different in case of ball-end milling. In case of horizontal surface, the effective diameter, based on Fig. 1, can be calculated by Eq. (1).

$$D_{eff} = 2 \cdot \sqrt{\left(\frac{D}{2}\right)^2 + \left(\frac{D}{2} - a_p\right)^2} \quad (1)$$

where as a_p is the depth of cut, and D is the cutter's nominal diameter.

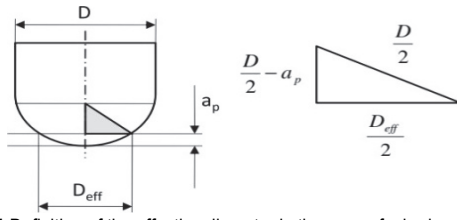


Figure 1 Definition of the effective diameter in the case of a horizontal plane.

However, as mentioned before, the cutting tool's diameter changes because of the change in the surface inclination, the different section of the tool's edge will work. Fig. 2 shows an inclined surface and a ball-end milling cutter.

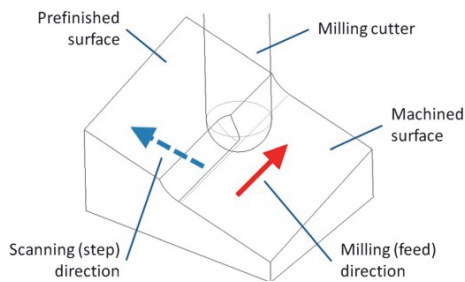


Figure 2 Ball-end milling of an inclined plane surface.

The working (effective) diameter can be defined as the distance of the intersection circle and the tool axis. The intersection circle is generated by the machined surface parallel surface, when the distance between surfaces is the depth of cut (a_p). Based on the geometric model of Mikó and Zentay [15] the intersection circle can be described. However, if the origin of the coordinate system is located to the centre of the ball, further transformation will be simpler. The equation of the intersection circle, when the surface is horizontal, can be described by Eq. (2).

The surface inclination can be described by the angular position of the normal vector. A_{N1} defines the angular position to the x axis, and A_{N2} to the z axis. Then two rotation operators are enough to calculate the current equation of the intersection circle.

The use of intersection plane instead of the offset surface results in easier calculation, but causes some differences in results.

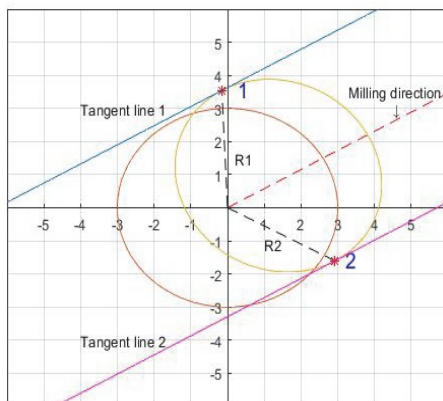


Figure 3 Tangent points on the transformed circle.

The current working diameter can be selected by considering the feed direction. The point has to be found, when the tangent plane, which perpendicular to the xy plane is parallel with the feed direction (Fig. 3). The central circle is the original section curve. The other one is the view of the transformed circle. The mathematical description of the transformed curve can be generated by two rotation matrices (Eq. (3) to Eq. (5)). On the transformed circle, two points can be defined by the tangent line, which has the same direction as the feed direction of the milling (A) (Eq. (6)).

$$\underline{C}_{r_{eff}} = \begin{bmatrix} R_{eff} \cdot \cos(2\pi t) \\ R_{eff} \cdot \sin(2\pi t) \\ -R + a_p \\ 1 \end{bmatrix}, t \in [0, 1] \quad (2)$$

$$\overline{\overline{Tr}} = \overline{\overline{F_2}} \cdot \overline{\overline{F_1}} \quad (3)$$

$$\overline{\overline{Tr}} = \overline{\overline{F_2}} \cdot \overline{\overline{F_1}} = \begin{bmatrix} \cos(A_{N1}) \cdot \cos(A_{N2}) & -\sin(A_{N1}) & -\cos(A_{N1}) \cdot \sin(A_{N1}) & 0 \\ \sin(A_{N1}) \cdot \cos(A_{N2}) & \cos(A_{N1}) & -\sin(A_{N1}) \cdot \sin(A_{N2}) & 0 \\ \sin(A_{N2}) & 0 & \cos(A_{N2}) & 0 \\ 0 & 0 & 0 & 1 \end{bmatrix} \quad (4)$$

$$\overline{\overline{C}}_{eff}^T = \overline{\overline{Tr}} \cdot \overline{\overline{C}}_{eff} = \begin{bmatrix} \cos(A_{N1}) \cdot \cos(A_{N2}) & -\sin(A_{N1}) & -\cos(A_{N1}) \cdot \sin(A_{N1}) & 0 \\ \sin(A_{N1}) \cdot \cos(A_{N2}) & \cos(A_{N1}) & -\sin(A_{N1}) \cdot \sin(A_{N2}) & 0 \\ \sin(A_{N2}) & 0 & \cos(A_{N2}) & 0 \\ 0 & 0 & 0 & 1 \end{bmatrix} \cdot \begin{bmatrix} R_{eff} \cdot \cos(2\pi t) \\ R_{eff} \cdot \sin(2\pi t) \\ (-R + a_p) \\ 1 \end{bmatrix} \quad (5)$$

$$\frac{d\overline{\overline{C}}_{eff}^T}{dt} = \text{tg}A$$

The location of the tangent point can be calculated by first differential of the curve:

$$\frac{d\overline{\overline{C}}_{eff}^T}{dt} = \text{tg}A \quad (6)$$

Considering the width of cut, the other 4 points can be defined, which indicate the starting or end point of the cutting (Fig. 5).

The step-over parameter (a_c) defines two additional points per sides, which depends on the milling process whether it is a down-milling or up-milling. By taking a parallel line to the tangent line with a distance equal to the width of cut, two points can be recognised on the transformed circle (Fig. 4).

Depending on the direction of width of cut, the milling cutter can work on the side 1 or side 2. In case of up-milling, the cutting cycle starts at point 1 and ends at point

1' as in Fig. 5a, whereas in the case of down-milling, the cutting process starts at point 1'' and ends at point 1 (Fig. 5b). If the tool works on the side 2, in case of down-milling the chip removal starts at point 2' and ends at point 2 (Fig. 5c), but in case of up-milling the chip removal there is between point 2 and 2'' (Fig. 5d)

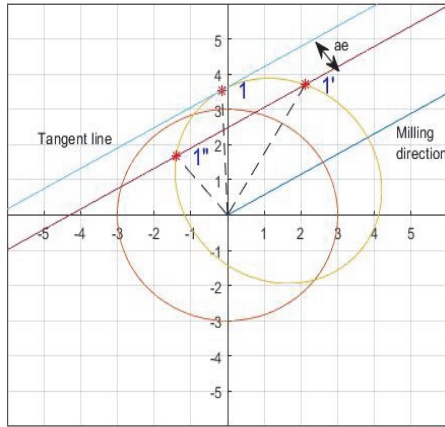


Figure 4 The extreme points defined by the width of cut

With a higher width of cut (a_e), the change in the effective diameter will increase. It means, the cutting speed changes during one chip removal process, which will affect the cutting speed and result in insufficient surface roughness.

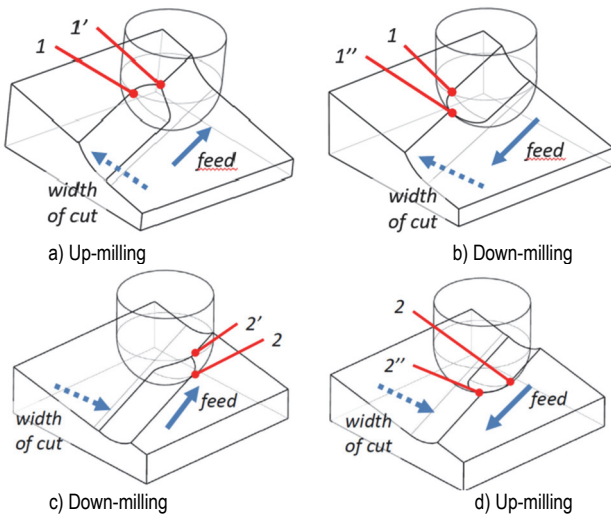


Figure 5 Extreme points

The simulation was implemented in Matlab. The pseudo-code of the Matlab program is the next:

- 1. Set the tool parameter: D_c .
- 2. Set the input cutting parameters A , a_e , a_p , n .
- 3. Set the surface inclination: A_{N1} , A_{N2} .
- 4. Calculate the effective diameter in horizontal plane.
- 5. Create the transformed circle considering the inclination of the surface.
- 6. Find the two tangent points (1, 2) when the slope of the tangent line is equal to the feed direction (A).
- 7. Find the parallel line to the tangent line with a distance equal to the width of cut.
- 8. Find the intersect between the transformed circle and the parallel line (1', 1'', 2', 2'').
- 9. Calculate the distance between the tangent points and the

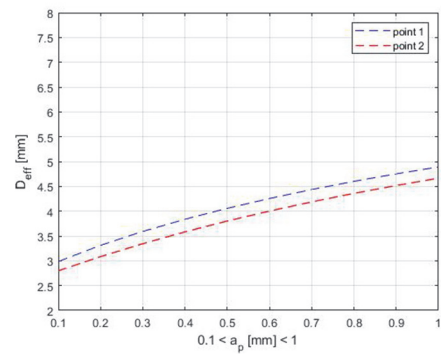
tool centre.

10. Calculate the distance between the tool centre and the intersecting points.

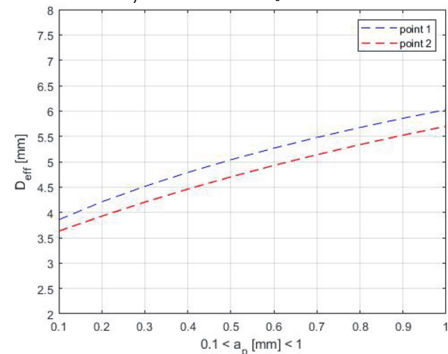
11. Output Working diameters: D_{eff} and current v_c .

3 THE EFFECT OF THE DEPTH OF CUT AND THE WIDTH OF CUT

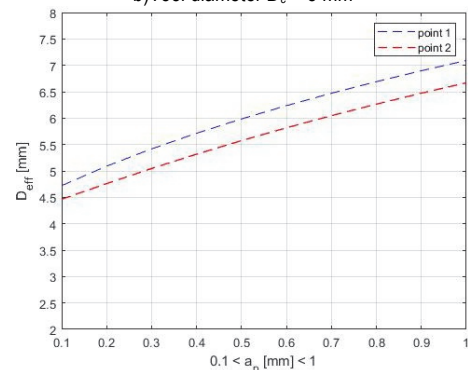
The cutting diameter depends on the tool diameter, the surface inclination and the depth of cut (a_p). The effect of them is investigated by simulations. First, the effect of the tool diameter, the depth of cut and the width of cut is presented in case of a particular surface position and feed direction. The values of the cutting and the tool parameters were determined based on the industrial practice in order to demonstrate the effect of the each parameter.



a) Tool diameter $D_c = 6$ mm



b) Tool diameter $D_c = 8$ mm



c) Tool diameter $D_c = 10$ mm

Figure 6 The effective diameter in the function of depth of cut.

The depth of cut or the axial depth of cut a_p represents the distance the tool engages into the workpiece in the z axis. Therefore, to increase the work done by the tool, a higher depth of cut should be defined. This can be noticed in Fig. 6, when the $A_{N1} = 35^\circ$, $A_{N2} = 25^\circ$ and $A = 30^\circ$. With increasing the depth of cut, the working diameter increases too. When the milling is performed from the bottom to the

top, the working diameter is larger. The difference depends on the inclination of the surface. The figure shows the effects of the depth of cut on the working diameter, using different tool diameters (6, 8 and 10mm). At $a_p = 0.1$ mm the tool works with half of its diameter.

Fig. 7 shows how the change in the width of cut a_c affects working diameter, in the case of up milling and down milling using different tool diameters (6, 8 and 10 mm), when $a_p = 1$ mm at cutting point 1.

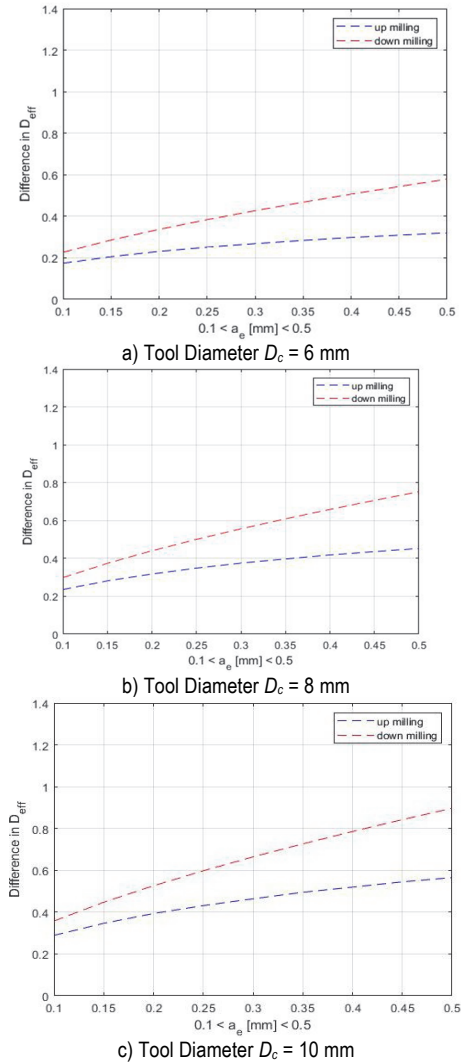


Figure 7 The change of the working diameter during chip removal in up and down milling at point 1.

As it can be seen in Fig. 7, the ranges of the change of working diameter are similar despite using different tool diameters, which is expected as increasing the nominal diameter of the tool will increase the working diameter but does not affect the change of the working diameter of the same tool. The change is related to the cutting parameters as depth and width of cut, mentioned before, and the surface inclination, which will be discussed in the next section.

4 THE EFFECT OF THE FEED DIRECTION

The working diameter is influenced by the feed direction too, so beside the tool diameter, the depth of cut, the width of cut and the surface inclination, the feed direction has to be considered. Fig. 8 shows the change of

the working diameter due to the change in the feed direction, with parameters as follows: $D_c = 10$ mm; $A_{N1} = 35^\circ$; $A_{N2} = 25^\circ$; $a_p = 1$ mm; $a_e = 1$ mm.

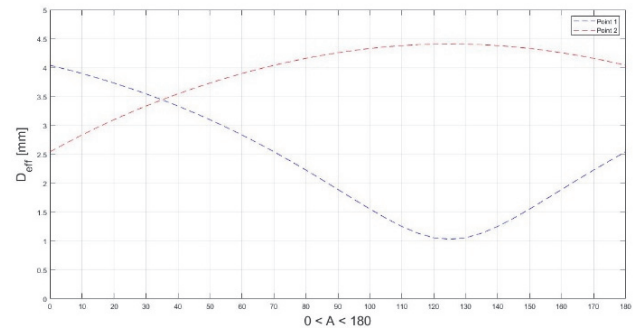


Figure 8 The effective diameter as a function of the feed direction ($a_p = 1$ mm)

The working diameter changes dramatically with the milling direction. This change is in the range of 2.5 - 4.5 mm for point 2, whereas the working diameter changes between 1 - 4 mm at point 1. The working diameter of point 1 at $A = 180^\circ$ is equal with the working diameter of point 2 at $A = 0^\circ$. If the angle of the feed direction is larger than 180° , the point 2 starts to work. In this simulation, the width of cut has not got a role.

If the depth of cut is 0.3 mm, which is a realistic data for machining, the character of the curves is the same, but the values are lower. The value of the effective diameter changes from 0.5 to 3.5 mm.

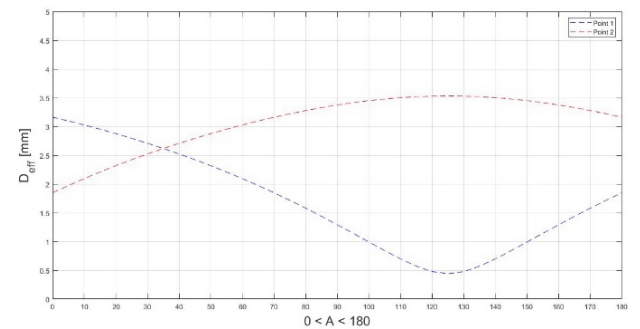


Figure 9 The effective diameter as a function of the feed direction ($a_p = 0.3$ mm)

Fig. 8 and Fig. 9 illustrate the importance of the proper feed direction to guarantee the minimum change in the working diameter. The presented diagram can be generated in every point of a surface, when the surface inclination is changed, and the best feed direction can be selected from the viewpoint of working diameter.

5 THE EFFECT OF THE SURFACE INCLINATION

As has been mentioned before, the working diameter changes during the milling process due to the change of the inclination of the surface (A_{N1} , A_{N2}). In this case study, the effect of the surface inclination is presented, and the changing of the cutting speed is presented too. During the simulation the tool diameter is 10 mm, the nominal cutting speed is $v_c = 120$ m/min, the spindle speed is $n = 3820$ 1/min.

Fig. 10 shows the changing of the working diameter of the ball-end mill, when the depth of cut is 1 mm and the feed direction is $A = 30^\circ$. The inclination of the surface has a significant effect on the working diameter, which shows

a big change from point to point. The changing of the surface normal vector (A_{N1} , A_{N2}) means changing the character of the surface. In Fig. 9a, the working diameter is calculated between the centre of the tool and point 1 on the transformed circle, whereas, in Fig. 9b, it is calculated between the centre of the tool and point 2 on the transformed circle. The lowest value 0.055 mm at $A_{N1} = 120^\circ$, $A_{N2} = -37.5^\circ$ in the case of points 1, and $A_{N1} = 120^\circ$, $A_{N2} = 37.5^\circ$ in the case of point 2. The highest diameter 4.950 mm at $A_{N1} = 120^\circ$, $A_{N2} = 45^\circ$ in the case of point 1, and $A_{N1} = 120^\circ$, $A_{N2} = -45^\circ$ in the case of point 2. The minimum and maximum values of the D_{eff_1} and D_{eff_2} are the same, the role of point 1 and 2 changes by the changing of A_{N1} and A_{N2} . The two diagrams are symmetrical to the axis A_{N1} .

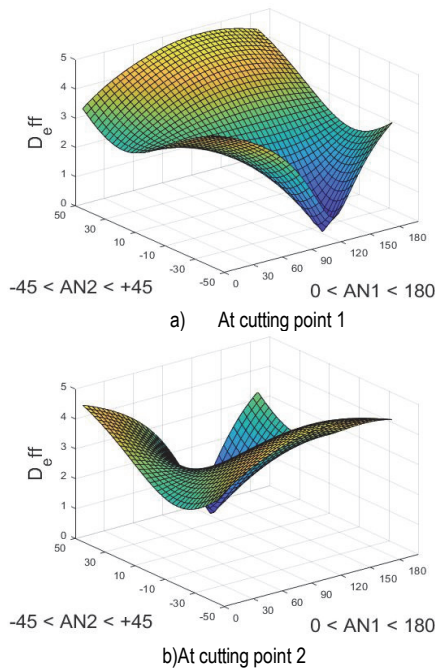


Figure 10 The change of the effective diameter as a function of the surface inclination ($A = 30^\circ$)

Fig. 11 shows how the cutting speed changes due to the change of the surface inclination, as the actual cutting speed that can be calculated depends on the effective diameter at each point using the formula:

$$v_c = \frac{D_{eff} \cdot n \cdot \pi}{1000} \tag{7}$$

Of course the location of the highest and the lowest cutting speed coincides with the location of the minimum and maximum value of the working diameter and the characters of the diagrams are similar to the diagrams of D_{eff} . In the case of point 1, the highest speed value is 59.4 mm/min at $A_{N1}=120^\circ$, $A_{N2}= 45^\circ$ and the lowest value is 0.66 mm/min at $A_{N1}=120^\circ$, $A_{N2}= -37.5^\circ$, in the case of point 2, we got the same highest and lowest value at $A_{N1}=120^\circ$, $A_{N2}= -45^\circ$ and at $A_{N1}=120^\circ$, $A_{N2}= 37.5^\circ$.

If the depth of cut is 0.3 mm, the working diameter is smaller, the character of the surface is similar to the previous result and the point 1 and point 2 surfaces are symmetric. Tab. 1 shows the data of the simulations.

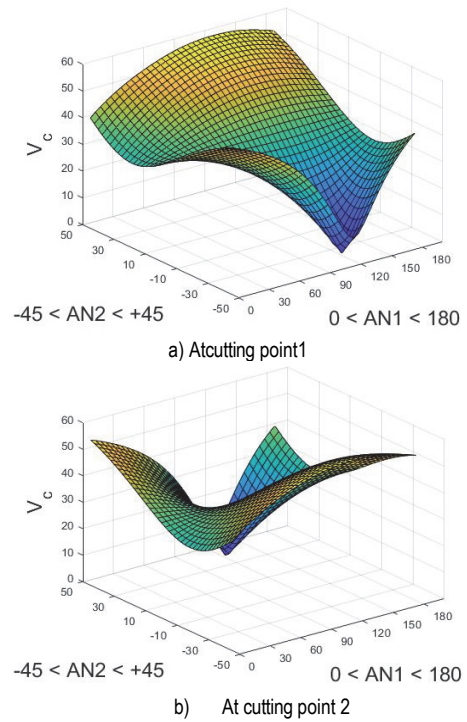


Figure 11 The change of the cutting speed as a function of the surface inclination ($A = 30^\circ$)

Table 1 The data of the simulation

$A / ^\circ$	30		60	
Cutting point	1	2	1	2
D_{effmin} / mm	0.005	0.005	0.005	0.005
$v_{cmin} / \text{m/min}$	0.06	0.06	0.06	0.06
$A_{N1} / ^\circ$	120	120	150	150
$A_{N2} / ^\circ$	-20	20	-20	20
D_{effmax} / mm	4.530	4.530	4.530	4.530
$v_{cmax} / \text{m/min}$	54.36	54.36	54.36	54.36
$A_{N1} / ^\circ$	120	120	150	150
$A_{N2} / ^\circ$	45	-45	45	-45

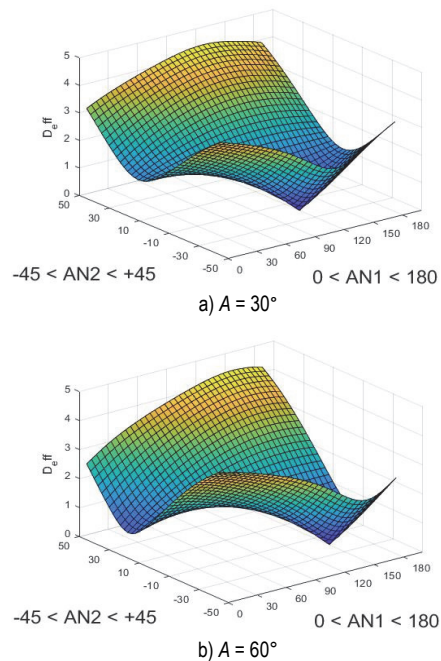


Figure 12 Working diameter at point 1, $a_p = 0.3 \text{ mm}$

In case of this simulation, the feed direction is different $A = 30^\circ$ and $A = 60^\circ$. The change of working diameter is presented in Fig. 12, the other diagrams can be seen in the

Appendix. These diagrams in the Appendix show the value of the working diameter and the cutting speed at points 1 and 2. The minimum value of the working diameter is 0.005 mm, and the maximum is 4.530 mm, which is smaller than in case of $a_p = 1$ mm. The minimum and maximum values are the same in both investigated cases, but the location of them is different. The surface of the diagram is shifted along A_{N1} with 30° . The cutting speed changes parallel with the working diameter in the range of 0.05 - 54.5 m/min.

Comparing the actual cutting speed with the nominal cutting speed, the effect of the surface inclination is noticeable, the highest value of the actual cutting speed equals half of the nominal cutting speed and at some point, the speed is too low, close to zero, which affects the roughness of the surface and its quality.

6 CONCLUSION

This work illustrates how the working diameter of the ball-end milling cutter changes due to the change of the surface inclination and the feed direction, affecting the homogeneity of the machined surface. Besides, it investigates the effect of the depth of cut and width of cut on the working diameter. The aim of the research is to create an optimization algorithm in order to improve the surface quality of milled free-form surface by the control of working diameter of the ball-end milling cutter.

Currently the result of the simulation was presented. The simulation model was developed to calculate the working diameter in general case. The geometric method [15] was used and modified in order to be easier implemented in Matlab environment. The simulation application ensured more detailed investigation of the each parameter. The steps of the simulation model, which has been implemented, are as follows:

- The intersect circle between the milling cutter and the surface is defined in the horizontal plane to calculate the theoretical effective diameter.
- The intersect circle can be transformed considering the surface inclination at the contact point.
- The distance between the center of the milling cutter and a point on the transformed circle represents the effective diameter at this point.
- The feed direction parallel tangent lines determines two points on the transformed circle, as the cutting points.
- The width of cut determines the other two points on the transformed circle as the starting or finishing point of the chip removal process.

The results give an insight into the impact of the cutting parameters on the effective diameter. Besides, they give a clear image of the effect of feed direction and the inclination of the surface on the effective diameter and the cutting speed. Using a relatively high value of depth of cut increases the effective diameter and achieves more engagement of the tool in the workpiece, but the load of the cutting tool increases too. While increasing the width of cut increases the change of the effective diameter along the chip removal section. Therefore, taking into consideration this parameter can help in reducing the change in the working diameter.

The impact of the feed direction and surface

inclination is demonstrated. However, while nothing can be done related to the surface inclination, the feed direction is the parameter that can be chosen carefully to achieve a constant working diameter. The change in the working diameter leads to a change in the real cutting speed, which will affect the changing of the surface roughness of the milled surface. Therefore, as a solution, the milling speed should be controlled and adjusted at each point to keep the cutting speed at the same value. During the optimization algorithm of the ball-end milling process, the working diameter has to be calculated point-by-point. The geometric information and the technological data are determined by the connection of the CAD model of the surface and the NC program.

The result of the simulation presents the importance of the effective diameter to the changing of the cutting speed considering the inclination of the surface and the feed direction. The developed simulation makes it possible to investigate the changing of the cutting speed during the chip removal section, and the simulation algorithm can be the core of the optimization solution. The control of the constant cutting speed, based on the presented simulation method, and the investigation of the surface roughness of the free form surface in different cutting condition are the goal for future work.

7 REFERENCES

- [1] Lasemi, A., Xue, D., & Gu, P. (2010). Recent development in CNC machining of freeform surfaces: a state-of-the-art review. *Computer-Aided Design*, 42(7), 641-654. <https://doi.org/10.1016/j.cad.2010.04.002>
- [2] Chang, L. (2016). A Parametric Design of Ball End Mill and Simulating Process. Concordia University
- [3] Yang, L., Zheng, M. L. (2017). Simulation and Analysis of Ball-End Milling of Panel Moulds Based on Deform 3D. *International Journal of Simulation Modelling*, 16(2), 343-356. [https://doi.org/10.2507/IJSIMM16\(2\)CO9](https://doi.org/10.2507/IJSIMM16(2)CO9)
- [4] Sekulic, M., Pejic, V., Brezocnik, M., Gostimirovic, M., & Hadzistevic, M. (2018). Prediction of surface roughness in the ball-end milling process using response surface methodology, genetic algorithms, and grey wolf optimizer algorithm. *Advances in Production Engineering & Management*, 13(1), 018-030. <https://doi.org/10.14743/apem2018.1.270>
- [5] de Lacalle, L. N. L., Campa, F. J., & Lamikiz, A. (2011). Milling. *Modern Machining Technology*, 213-303. <https://doi.org/10.1533/9780857094940.213>
- [6] Kang, W. T., Derani, M. N., & Ratnam, M. M. (2020). Effect of Vibration on Surface Roughness in Finish Turning: Simulation Study. *International Journal of Simulation Modelling*, 19(4), 595-606. <https://doi.org/10.2507/IJSIMM19-4-531>
- [7] Fan, J. (2014). Cutting speed modelling in ball nose milling applications. *The International Journal of Advanced Manufacturing Technology*, 73(1-4), 161-171. <https://doi.org/10.1007/s00170-014-5672-3>
- [8] de Souza, A. F., Diniz, A. E., Rodrigues, A. R., & Coelho, R. T. (2014). Investi- gating the cutting phenomena in free-form milling using a ball-end cutting tool for die and mold manufacturing. *The International Journal of Advanced Manufacturing Technology*, 71(9-12), 1565-1577. <https://doi.org/10.1007/s00170-013-5579-4>
- [9] Wieczorowski, M., Wojciechowski, S., & Twardowski, P. (2014) Surface texture analysis after ball end milling with various surface inclination of hardened steel. *Metrology and Measurement Systems*, 21(1), 145-156.

<https://doi.org/10.2478/mms-2014-0014>

[10] Ižol, P., Tomáš, M., & Beňo, J. (2016). Milling strategies evaluation when simulating the forming dies' functional surfaces production. *Open Engineering*, 6(1). <https://doi.org/10.1515/eng-2016-0013>

[11] Buj-Corral, I., Ortiz-Marzo, J.-A., Costa-Herrero, L., Vivancos-Calvet, J., & Luis-Pérez, C. (2019). Optimal machining strategy selection in ball-end milling of hardened steels for injection molds. *Materials*, 12(6), 860. <https://doi.org/10.3390/ma12060860>

[12] Belguith, R., Khlifi, H., Saï, L., Baili, M., Dessein, G., & Saï, W. (2019). Effects of the Tool Bending on the Cutting Force in Ball End Milling. *Advances in Mechanical Engineering and Mechanics -CoTuMe 2018*, 143-151. https://doi.org/10.1007/978-3-030-19781-0_18

[13] Huo, G., Jiang, X., Su, C., Lu, Z., Sun, Y., Zheng, Z., & Xue, D. (2019). CNC tool path generation for freeform surface machining based on preferred feed direction field. *International Journal of Precision Engineering and Manufacturing*, 20(5), 777-790. <https://doi.org/10.1007/s12541-019-00084-2>

[14] Seikh, A. H., Mandal, B. B., Sarkar, A., Baig, M., Alharthi, N., & Alzahrani, B. (2019). Application of response surface methodology for prediction and modeling of surface roughness in ball end milling of OFHC copper. *International*

Journal of Mechanical and Materials Engineering, 14(1), 1-11. <https://doi.org/10.1186/s40712-019-0099-0>

[15] Mikó, B. & Zentay, P. (2019). A geometric approach of working tool diameter in 3-axis ball-end milling. *The International Journal of Advanced Manufacturing Technology*, 104(1-4), 1497-1507. <https://doi.org/10.1007/s00170-019-03968-9>

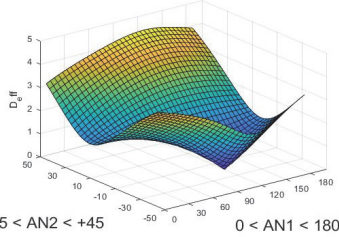
Contact information:

Abdulwahab MGHHERONY, PhD student
 (Corresponding author)
 Óbuda University,
 Bánki Donát Faculty of Mechanical and Safety Engineering,
 H-1081 Budapest Népszínház u. 8, Hungary
 E-mail: mgherony.abdulwhab@uni-obuda.hu

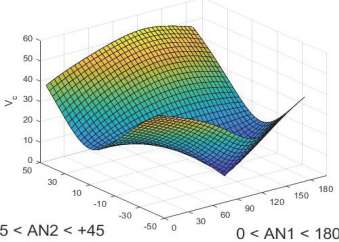
Balázs MIKÓ, Dr. Associate Professor
 Óbuda University,
 Bánki Donát Faculty of Mechanical and Safety Engineering,
 H-1081 Budapest Népszínház u. 8, Hungary
 E-mail: miko.balazs@bkgk.uni-obuda.hu

Appendix

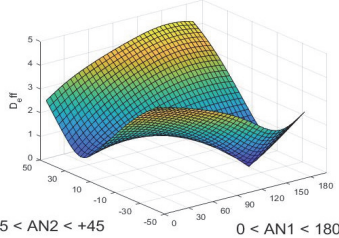
Working diameter at cutting point 1 $a_p = 0.3 \text{ mm}$ $A = 30^\circ$



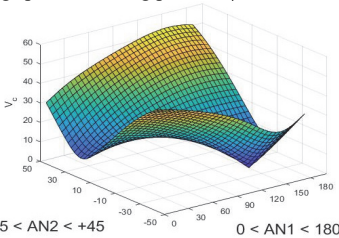
Cutting speed at cutting point 1 $a_p = 0.3 \text{ mm}$ $A = 30^\circ$



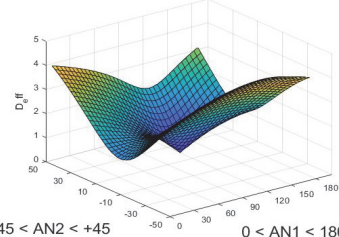
Working diameter at cutting point 1 $a_p = 0.3 \text{ mm}$ $A = 60^\circ$



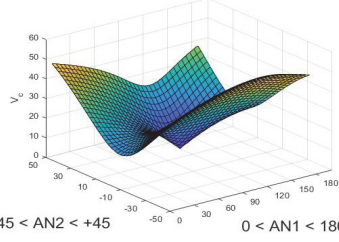
Cutting speed at cutting point 1 $a_p = 0.3 \text{ mm}$ $A = 60^\circ$



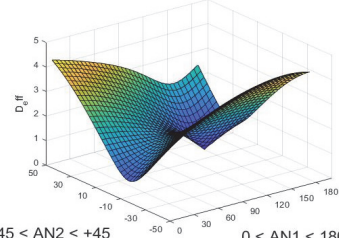
Working diameter at cutting point 2 $a_p = 0.3 \text{ mm}$ $A = 30^\circ$



Cutting speed at cutting point 2 $a_p = 0.3 \text{ mm}$ $A = 30^\circ$



Working diameter at cutting point 2 $a_p = 0.3 \text{ mm}$ $A = 60^\circ$



Cutting speed at cutting point 2 $a_p = 0.3 \text{ mm}$ $A = 60^\circ$

